Nuclear structure study of ^{20}Ne, ^{24}Mg, ^{28}Si and ^{32}S nuclei using Skyrme-Hartree-Fock method

Ahmed N. Abdullah

Department of Physics, College of Science, University of Baghdad, Baghdad, Iraq

E-mail: Ahmednajim1979@yahoo.com

Abstract

The Skyrme–Hartree–Fock (SHF) method with the Skyrme parameters; SKxtb, SGII, SKO, SKxs15, SKxs20 and SKxs25 have been used to investigate the ground state properties of some 2*s*-1*d* shell nuclei with *Z*=*N* (namely; ^{20}Ne, ^{24}Mg, ^{28}Si and ^{32}S) such as, the charge, proton and matter densities, the corresponding root mean square (rms) radii, neutron skin thickness, elastic electron scattering form factors and the binding energy per nucleon. The calculated results have been discussed and compared with the available experimental data.

Key words

Electron scattering, Skyrme–Hartree–Fock (SHF) method, sd-shell nuclei.

Article info.

Received: Nov. 2016
Accepted: Jan. 2017
Published: Mar. 2017

دراسة التركيب النووي للنوى ^{20}Ne، ^{24}Mg، ^{28}Si و ^{32}S باستخدام طريقة سكيرم- هارتري- فوك

أحمد نجم عبدالله

قسم الفيزياء، كلية العلوم، جامعة بغداد، بغداد، العراق

الخلاصة

تم استخدام طريقة سكيرم- هارتري- فوك مع برامترات مختلفة هي SKxtb, SGII, SKO, SKxs15, SKxs20, SKxs25 لدراسة خصائص الحالة الارضية لنوى واقعة ضمن القشرة النووية 2*s*-1*d* يكون فيها عدد البروتونات (Z) مساوياً الى عدد النيوترونات (N) (مثل النوى ^{20}Ne، ^{24}Mg، ^{28}Si و^{32}S) مثل كثافة كل من الشحنة، البروتون والكتلة مع انصاف الاقطار المرافقة لها، بالاضافة الى حساب السمك النيوتروني، عوامل التشكل للاستطارة الالكترونية المرنة ومعدل طاقة الربط النووية. لقد تمت مقارنة النتائج النظرية مع نظيراتها من القيم العملية المتاحة.

Introduction

The electron scattering from the nucleus at high energy gives important information about the nuclear structure. Information obtained from the high energy electron scattering by the nuclei depends on the magnitude of the de Broglie wave length that is associated with the electron which is compared with the range of the nuclear forces. When the energy of the incident electron is in the range of 100 MeV and more, the de Broglie wave length will be in the range of the spatial extension of the target nucleus. Thus with this energy, the electron represents a best probe to study the nuclear structure [1]. The nuclear charge radius is one of the most obvious and important nuclear parameters that give information about the nuclear shell model and the influence of effective interactions on nuclear structure. Experimental information on root-mean square (rms) nuclear charge radii can be derived from different sources and has been published several times. The results

from electron scattering experiments are expressed in terms of the (rms) radius, and for some nuclei, in parameters of the Fermi-Dirac distribution [2].

The Hartree-Fock method with an effective interaction with Skyrme forces is widely used for studying the properties of nuclei. This method allows possibility to calculate many aspects of nuclei by means of quantum mechanical methods in microscopic scale. Especially the method is successfully used for a wide range of nuclear characteristics such as binding energy, rms charge radii, neutron and proton density, electromagnetic multipole moments, etc. The Hartree-Fock description of nuclear properties yields good results not only for stable even-even spherical and deformed nuclei, but also for neutron-rich and neutron -deficient nuclei [3]. Aytekin [4] has been calculated the proton, neutron and charge densities, the corresponding rms nuclear radii and neutron skin thickness for the neutron-rich Ni, Kr and Sn isotopes by the Hartree-Fock method with an effective Skyrme force based on nucleon-nucleon interactions known as SI, SIII, SVI, T3, SKM and SKM*. The results obtained via theoretical approach were close to experimental observations. Tel [5] has been calculated the neutron and proton densities, rms charge radii, neutron radii, mass radii and neutron skin thickness for $^{8-18}$Be isotopes nuclei. The results obtained were compared with the experimental and theoretical results of other researchers by using Hartree–Fock method with an effective interaction with Skyrme forces.

In this research, we investigate the ground state features of ^{20}Ne, ^{24}Mg, ^{28}Si and ^{32}S nuclei using the Skyrme–Hartree–Fock (SHF) method with the Skyrme parameters; SKxtb [6], SGII [7], SKO [8], SKxs15, SKxs20 and SKxs25 [9] and compared the obtained results with the available experimental data.

Theory

The effective interaction proposed by Skyrme was designed for Hartree–Fock (HF) calculations of nuclei. It basically consists of a two-body term which is momentum dependent, and a zero range three-body term [10]:

$$V_{CS} = \sum_{i<j} V_{ij}^{(2)} + \sum_{i<j<k} V_{ijk}^{(3)} \qquad (1)$$

with

$$V_{ij}^{(2)} = t_0(1 + x_0 p_\sigma)\delta(\vec{r}) + \frac{1}{2}t_1\left[\delta(\vec{r})\vec{k}^2 + \vec{k}'^2\delta(\vec{r})\right] + t_2\overrightarrow{k'}.\delta(\vec{r})\vec{k} + it_4\left(\vec{\sigma}_i - \vec{\sigma}_j\right).\vec{k} \times \delta(\vec{r})\vec{k}, \qquad (2)$$

$$V_{ijk}^{(3)} = t_3\delta\left(\vec{r}_i - \vec{r}_j\right)\delta\left(\vec{r}_j - \vec{r}_k\right). \qquad (3)$$

The application of the Skyrme force in the field of low energy nuclear physics has been greatly motivated by the classical work of Vautherin and Brink [11]. In the HF calculations, the three-body term in (1) can be replaced with a density-dependent two-body term [11]:

$$V_{ijk}^{(3)} \cong V_{ij}^{(2)} = \frac{1}{6}t_3\rho\left(\vec{R}\right)\delta(\vec{r}), \qquad (4)$$

where

$\vec{R} = \left(\vec{r}_i + \vec{r}_j\right)/2$ and $\vec{r} = \left(\vec{r}_i - \vec{r}_j\right)$,

the relative momentum operators $\hat{k} = \left(\nabla_i - \nabla_j\right)/2i$ and $\hat{k'} = -\left(\nabla_i - \nabla_j\right)/2i$ are acting to the right and to the left, respectively [10].

The Skyrme forces are unified in a single form as an extended Skyrme force [12]

$$V_{Skyrme} = \sum_{i<j} V_{ij} = t_0(1 + x_0P_\sigma)\delta(\vec{r}) + \frac{t_1}{2}(1 + x_1P_\sigma)\left[\delta(\vec{r})\vec{k}^2 + \vec{k}'^2\delta(\vec{r})\right] + t_2(1 + x_2P_\sigma)\vec{k'}.\delta(\vec{r})\vec{k} + \frac{1}{6}t_3(1 + x_3P_\sigma)\rho^\alpha(\vec{R})\delta(\vec{r}) + it_4\vec{k}'.\delta(\vec{r})(\vec{\sigma}_i + \vec{\sigma}_j) \times \vec{k}\,, \quad (5)$$

where P_σ is the space exchange operator, $\delta(\vec{r})$ is the delta function, $\vec{k}$ is the relative momentum, $\vec{\sigma}$ is the vector of Pauli spin matrices and t_0, t_1, t_2, t_3, t_4, x_0, x_1, x_2, x_3, and α are Skyrme force parameters.

The proton and neutron densities are given in terms of a few nucleon densities [5]:

$$\rho_g(\vec{r}) \sum_{\beta \in g} w_\beta \psi_\beta^+(\vec{r})\, \psi_\beta(\vec{r}), \quad (6)$$

where g denotes the proton or neutron, ψ_β is the single-particle wave function of the state β and w_β represents the occupation probability of the state β.

To compute the observable charge density from the Hartree–Fock results, one has to take into account that the nucleons themselves have an intrinsic electromagnetic structure [13] Thus one needs to fold the proton and neutron densities from the Hartree–Fock method with the intrinsic charge density of the nucleons. Folding becomes a simple product in Fourier space, so the densities are transformed to the so-called form factors:

$$F_k(q) = 4\pi \int_0^\infty r^2 j_0(qr)\, \rho_k(r)\, dr \quad (7)$$

where j_0 is the spherical Bessel function of the zeroth order.

The root mean square (rms) radii of the neutron, proton and charge densities can be obtained from these densities as follows [10]

$$r_g = \langle r_g^2 \rangle^{1/2} = \left[\frac{\int r^2 \rho_g(r) dr}{\int \rho_g(r) dr}\right]^{1/2} \qquad g = n, p, c \quad (8)$$

The neutron skin thickness *t*, is defined as:

$$t = r_n - r_p \quad (9)$$

Results and discussions

The Skyrme-Hartree-Fock (SHF) method has been employed to study the ground state properties of ^{20}Ne, ^{24}Mg, ^{28}Si and ^{32}S nuclei including the proton, charge and matter densities, charge, proton, neutron and matter rms radii, neutron skin thickness, the binding energies per nucleon and elastic charge form factors. The Skyrme force parameters that have been used in the present study are given in Table 1.

Table 1: The parameters of Skyrme force used in the present calculations.

Parameter	SKxtb [6]	SGII [7]	SKO [8]	SKxs15 [9]	SKxs20 [9]	SKxs25 [9]
t_0 (MeV.fm^3)	-1446.759	-2645.0	-2103.7	-2883.294	-2885.239	-2887.813
t_1 (MeV.fm^5)	250.852	340.0	303.4	291.598	302.733	315.504
t_2 (MeV.fm^5)	-132.993	-41.9	791.7	-314.892	-323.419	-329.305
t_3 (MeV.fm$^{3\alpha}$)	12127.649	15595.0	13553.0	18239.547	18237.492	18229.807
t_4 (MeV.fm^5)	153.054	105.0	118.0	161.351	162.726	163.933
x_0	0.329	0.09	-0.21	0.476	0.137	-0.186
x_1	0.518	-0.059	-2.81	-0.254	-0.255	-0.248
x_2	0.139	1.425	-1.46	-0.611	-0.607	-0.601
x_3	0.018	0.06	-0.43	0.529	0.054	-0.409
α	0.5	0.167	0.25	0.167	0.167	0.167

The calculated charge rms radii for ^{20}Ne, ^{24}Mg, ^{28}Si and ^{32}S nuclei using different Skyrme parameters along with those of RMFT [14] and experimental [2] results are listed in Table 2. It can be shown that the charge rms radii are increased from (2.900-2.980) fm for ^{20}Ne to (3.239-3.292) fm for ^{32}S as the proton number increases. Also, the calculated charge rms radii of ^{20}Ne, ^{24}Mg and ^{28}Si with SKxs25 parameter are more close to the experimental data than other parameters. In case of ^{32}S, analysis shows that the calculated charge rms radii with SKO parameter are in excellent agreement with the experimental data. Besides, the calculated charge rms radii for selected nuclei are more close to the experimental results than those of RMFT results.

The calculated results of the proton and neutron rms radii for selected nuclei with different Skyrme parameters are tabulated in Tables 3 and 4, respectively. For comparison the results of RMFT [14] are also given in these tables. Our analyses show that the values of these rms radii increase with the increasing of proton number. On the other hand, the calculated proton and neutron rms radii of ^{20}Ne, ^{24}Mg and ^{28}Si obtained by SKxs25 parameter are more close to the RMFT results than other parameters. In case of ^{32}S nucleus, the calculated proton rms radius obtained with SGII parameter is closer to the RMFT results, whereas the neutron rms radius calculated with SKxs20 parameter is in well agreement with the RMFT results. The neutron skin thickness is calculated as the differences of neutron and proton rms radii obtained with SKxs25 parameter is also shown in Table 4. It has been shown from Table 4 that the neutron skin thickness t values have decreased from (-0.049) fm for ^{20}Ne to (-0.062) fm for ^{32}S by increasing the proton number. Finally, the matter rms radii with different Skyrme parameters have been calculated for nuclei under study and given in Table 5. It has been shown from Table 5 that the values of matter rms radii have approximately been increased from (2.807-2.882) fm for ^{20}Ne to (3.136-3.179) fm for ^{32}S with the increasing of the number of proton.

Table 2: Calculated charge rms radii compared with RMFT and experimental results.

Nuclei	SKxtb	SGII	SKO	SKxs15	SKxs20	SKxs25	RMFT [14]	Exp. [2]
^{20}Ne	2.900	2.933	2.915	2.958	2.968	2.980	3.020	2.992
^{24}Mg	3.014	3.038	3.014	3.058	3.068	3.079	3.126	3.080
^{28}Si	3.108	3.116	3.093	3.138	3.146	3.158	3.177	3.154
^{32}S	3.251	3.271	3.239	3.273	3.281	3.292	3.282	3.239

Table 3: Calculated proton rms radii compared with RMFT results.

Nuclei	SKxtb	SGII	SKO	SKxs15	SKxs20	SKxs25	RMFT [14]
^{20}Ne	2.824	2.858	2.840	2.884	2.894	2.906	2.911
^{24}Mg	2.930	2.955	2.931	2.976	2.986	2.998	3.021
^{28}Si	3.022	3.030	3.006	3.138	3.062	3.073	3.075
^{32}S	3.167	3.188	3.155	3.190	3.199	3.210	3.183

Table 4: Calculated neutron rms radii compared with RMFT results.

Nuclei	SKxtb	SGII	SKO	SKxs15	SKxs20	SKxs25	RMFT [14]	*t* (SKxs25)
^{20}Ne	2.789	2.822	2.814	2.841	2.848	2.857	2.871	-0.049
^{24}Mg	2.893	2.918	2.904	2.932	2.939	2.948	2.983	-0.050
^{28}Si	2.984	2.991	2.979	3.006	3.013	3.022	3.036	-0.051
^{32}S	3.117	3.136	3.117	3.132	3.139	3.148	3.139	-0.062

Table 5: Calculated matter rms radii.

Nuclei	SKxtb	SGII	SKO	SKxs15	SKxs20	SKxs25
^{20}Ne	2.807	2.840	2.827	2.863	2.871	2.882
^{24}Mg	2.912	2.937	2.917	2.954	2.962	2.973
^{28}Si	3.003	3.011	2.993	3.030	3.038	3.048
^{32}S	3.142	3.162	3.136	3.161	3.169	3.179

Fig. 1 shows the calculated charge density distributions for ^{20}Ne [Fig.1(a)], ^{24}Mg [Fig. 1(b)], ^{28}Si [Fig. 1(c)] and ^{32}S [Fig. 1(d)] nuclei obtained by SKxs25 Skyrme parameter along with the fitted to the experimental data (denoted by filled circle symbols) [2]. One can see from this figure that the calculated charge density distributions are in very good agreement with those fitted to the experimental data except a slight deviation appearing in the calculated results at the region of small *r*.

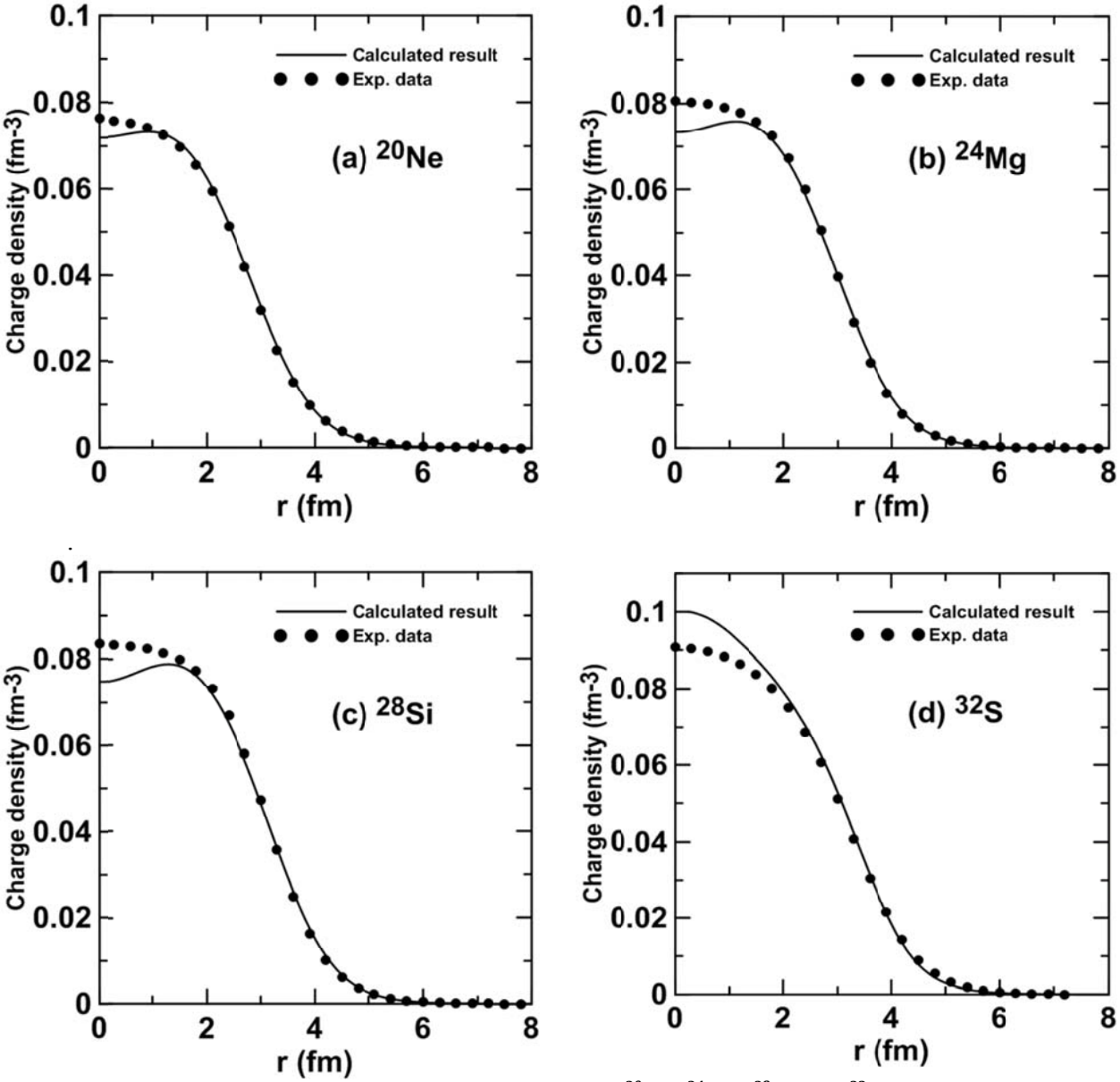

Fig. 1: Calculated charge density distributions for ^{20}Ne, ^{24}Mg, ^{28}Si and ^{32}S nuclei obtained by SKxs25 parameter compared with the fitted to the experimental data [2].

The charge and proton densities for the ^{20}Ne, ^{24}Mg, ^{28}Si and ^{32}S nuclei using the SKxs25 are shown in Figs. 2 (a) and (b), respectively. The obtained values of the charge density for the ^{20}Ne, ^{24}Mg and ^{28}Si nuclei at the center (r = 0) have approximately increased from (0.072 fm^{-3}) for ^{20}Ne to (0.075 fm^{-3}) for ^{28}Si with increasing proton number. On the other hand, the proton densities for these nuclei, in the center, have remained approximately constant at about 0.069–0.07 fm^{-3} as shown in Fig. 2 (b). The charge and proton densities for ^{32}S nucleus have, respectively, 0.096 fm^{-3} and 0.1 fm^{-3} central values, which are higher than that of the other nuclei. Moreover, the charge and proton densities for ^{20}Ne, ^{24}Mg and ^{28}Si nuclei have a maximum value at about 1.0 - 1.3 fm, while these densities for ^{32}S nucleus have a maximum value at the center. Furthermore, the charge and proton densities for nuclei under investigation show the same behavior after r =2 fm and approaches to zero at the distance of 6 fm.

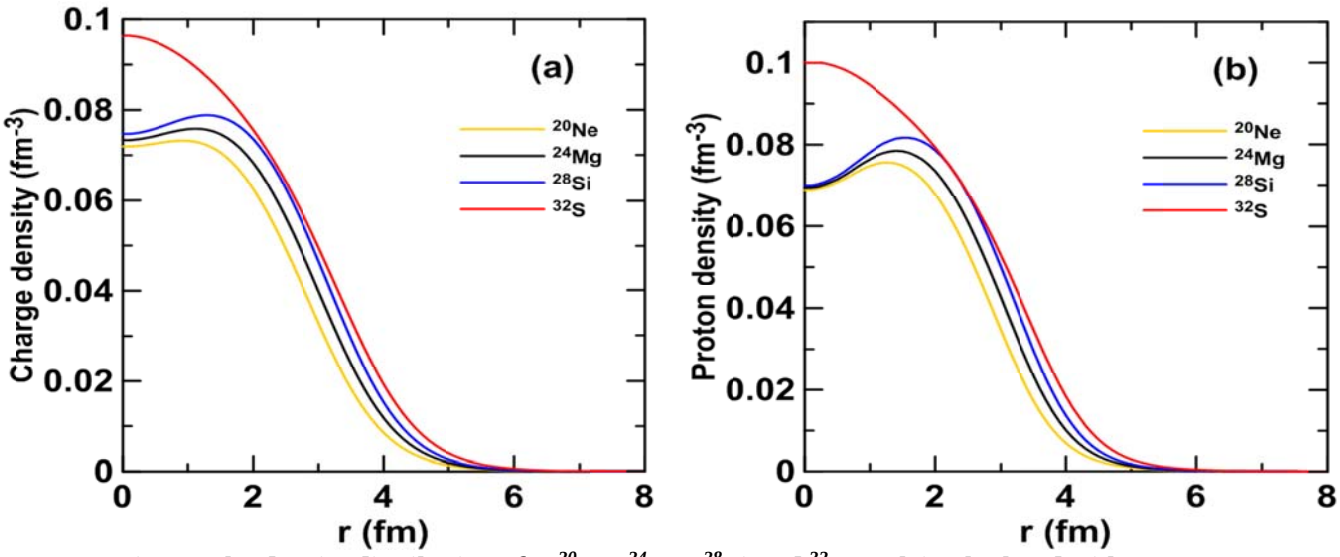

Fig. 2: The density distributions for ^{20}Ne, ^{24}Mg, ^{28}Si and ^{32}S nuclei calculated with SKxs25 parameters; (a) charge and (b) proton.

Figs. 3(a) and 3(b) illustrate the evaluated results of matter density distributions for ^{20}Ne, ^{24}Mg, ^{28}Si and ^{32}S nuclei obtained by SHF method with SKxs25 parameter. For comparison the fitted to the experimental matter densities of these nuclei [2] are also shown in Fig. 3(a). We have clearly shown from Fig. 3(a) that the calculated matter density distributions for ^{20}Ne, ^{24}Mg and ^{28}Si nuclei underestimate those fitted to the experimental data at the central region and the calculated results for ^{32}S nucleus overestimate the fitted to the experimental data at this region, whereas beyond this region the calculated results of these nuclei agree very well with the fitted data. Also, one can see from Fig. 3(b) that ^{20}Ne, ^{24}Mg and ^{28}Si nuclei have the maximum densities at about 1.3-1.6 fm, while ^{32}S has maximum density at the center.

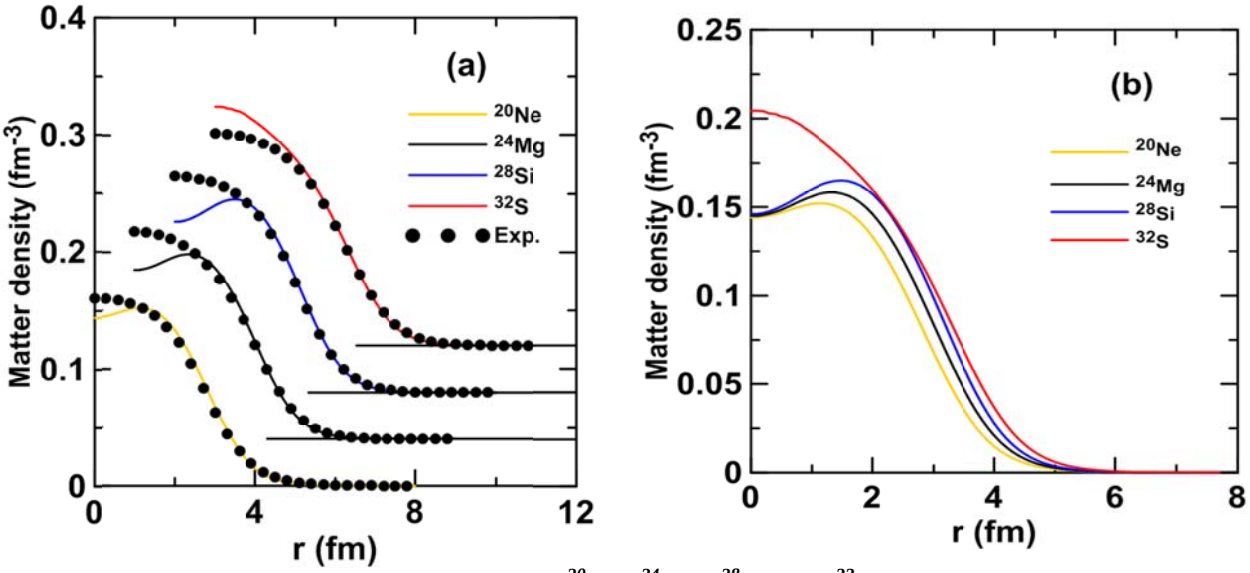

Fig. 3: Matter density distributions for ^{20}Ne, ^{24}Mg, ^{28}Si and ^{32}S nuclei calculated with SKxs25 parameters. In Fig. 3 (a) the curves and data have been progressively offset by 1 fm and 0.04 in the matter density. The filled circle symbols are those fitted to the experimental data of ref [2].

The obtained binding energies per particle using Skyrme– Hartree–Fock method are presented in Table 6. According to these results, the calculated binding energy of ^{20}Ne for SGII parameter is closer to experimental data [15] than other interactions. In case of ^{24}Mg and ^{28}Si the binding energies with SKO parameter are more close to the experimental results [15]. Moreover, the binding energy of ^{32}S obtained by SKxs25 parameter is in a good agreement with experimental data [15].

Table 6: Calculated binding energy per nucleon along with experimental and RMFT results.

Nuclei	SKxtb	SGII	SKO	SKxs15	SKxs20	SKxs25	RMFT [14]	Exp. [15]
^{20}Ne	7.526	7.773	7.696	7.576	7.536	7.449	7.775	8.032
^{24}Mg	7.769	7.924	7.946	7.810	7.774	7.739	8.104	8.260
^{28}Si	8.254	8.400	8.465	8.294	8.261	8.227	8.293	8.447
^{32}S	8.367	8.530	8.600	8.481	8.456	8.430	8.318	8.439

The elastic electron scattering form factors of ^{20}Ne, ^{24}Mg, ^{28}Si and ^{32}S nuclei are presented in Figs. 4(a) to 4(d), respectively. As we can see from Fig.4 (a) that the available data of ^{20}Ne nucleus are restricted for a small region of momentum transfer $q \leq$ 1.2fm^{-1}. It is obvious from this figure that the calculated results are in excellent agreement with those of experimental data [16]. In ^{24}Mg, ^{28}Si and ^{32}S nuclei, the calculated form factors are in a satisfactory description with that of the experimental data [17] up to momentum transfer of q=2.3 fm^{-1} and discredit these data at higher momentum transfer (i.e. q > 2.2 fm^{-1}). Besides, the location of the observed first diffraction minimum suits very well with that of calculated results.

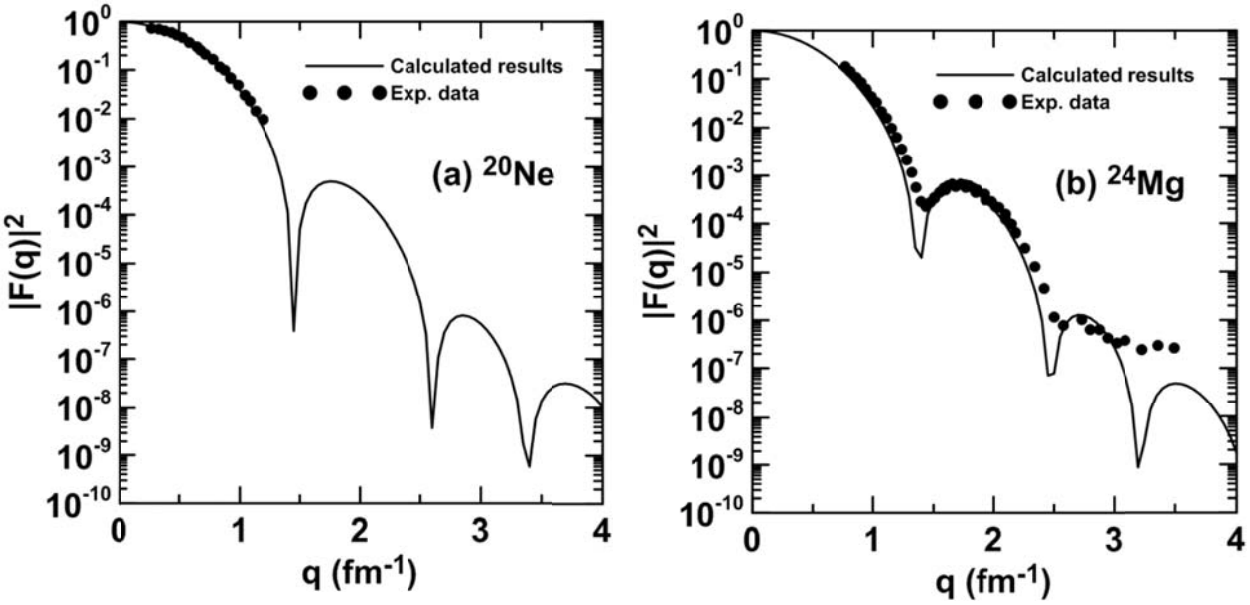

Fig. 4: Elastic charge form factors for ^{20}Ne, ^{24}Mg, ^{28}Si and ^{32}S nuclei obtained by SKxs25 parameter. The filled circle symbols are the experimental data of Ref. [16] for ^{20}Ne nucleus and Ref. [17] for ^{24}Mg, ^{28}Si and ^{32}S nuclei.

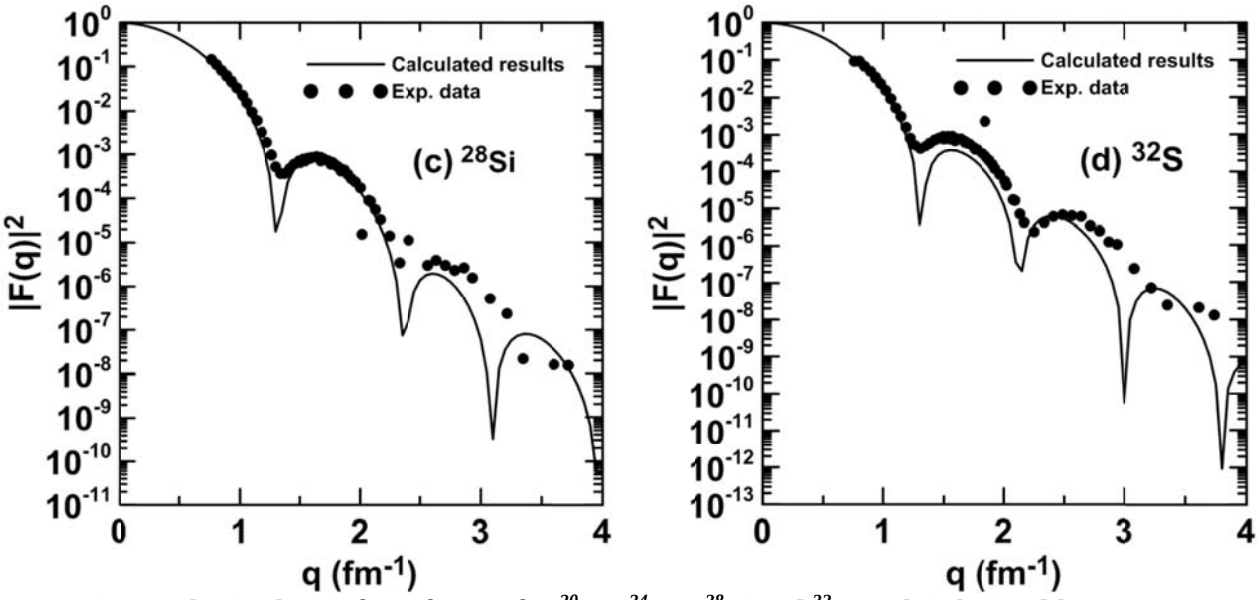

Fig. 4: Elastic charge form factors for ^{20}Ne, ^{24}Mg, ^{28}Si and ^{32}S nuclei obtained by SKxs25 parameter. The filled circle symbols are the experimental data of Ref. [16] for ^{20}Ne nucleus and Ref. [17] for ^{24}Mg, ^{28}Si and ^{32}S nuclei.

Summary and conclusions

In this research, the charge, proton and matter densities, charge, proton, neutron and matter root mean square (rms) radii, neutron skin thickness, elastic charge form factor and the binding energy per nucleon were calculated for ^{20}Ne, ^{24}Mg, ^{28}Si and ^{32}S nuclei. The results can be summarized and concluded as follows:

1- The calculated charge rms radii of ^{20}Ne, ^{24}Mg and ^{28}Si with SKxs25 parameter are more close to the experimental data than other parameters. While in ^{32}S, the calculated charge rms radii with SKO parameter are in excellent agreement with the experimental data. Furthermore, the calculated charge rms radii for these nuclei are more close to the experimental results than those of RMFT results.

2- The calculated proton, neutron and matter rms radii of nuclei under study have been increased with the increasing of proton number.

3- The calculated charge and matter density distributions for selected nuclei obtained by SKxs25 Skyrme parameter are in very good agreement with those fitted to experimental data except a slight deviation appearing in the calculated results at the region of small *r*.

4- In the description of the binding energies, while the SGII parameters work well for ^{20}Ne nucleus, the SKO parameters work well for ^{24}Mg and ^{28}Si nuclei. On the other hand, the best binding energy is obtained for ^{32}S nucleus with that of SKxs25.

5- The Skyrme-Hartree–Fock method is powerful tool in the investigation of nuclear structure of the spherical nuclei because this force is central and has zero range interactions. This means that the interactions are only dependence of radial and there is not dependence of angular.

References

[1] R. Roy and B. P. Nigam; "Nuclear Physics: Theory and Experiment", John and Sons, New York (1967).

[2] H. de Vries, C.W. de Jager, C. De Vries, Atomic Data and Nucl. Data Tables 36, (1987) 495-536.

[3] E. Tel, S. Okuducu, G. Tanır, N. N. Aktı, M. H. Bolukdemir, Commun.

Theor. Phys. (Beijing, China) 49 (2008) 696–702.
[4] H. Aytekin, E. Tel, R. Baldik, Turk. J. Phys., 32 (2008) 181-191.
[5] E. Tel, N. N. Aktı, S. Okuducu, A. Aydin, M. Sahan, F. A. Ugur, H. Sahan, J. Fusion Energy, 30 (2011) 58-63.
[6] B. A. Brown, T. Duguet T., Otsuka, D. Abe, T. Suzuki, Phys. Rev., C 74 (2006) 1-5.
[7] N. V. Giai and H. Sagawa, Phys. Lett., 106 B (1981) 379-382.
[8] P.-G. Reinhard D. J. Dean, W. Nazarewicz, J. Dobaczewski, J. A. Maruhn, M. R. Strayer, Phys. Rev., C 60 (1999) 1-20.
[9] B. A. Brown, G. Shen, G. C. Hillhouse, J. Meng, A. Trzcinska, Phys. Rev., C 76 (2007) 1-5.
[10] L. G. Qiang, J. Phys. G. Nuclear and Particle Physics, 17 (1991) 1-34.
[11] D. Vautherin and D. M. Brink, Phys. Rev., C5 (1972) 626-647.
[12] L. X. Ge, Y. Z. Zhuo, W. Norenberg, Nucl. Phys., A 459 (1986) 77-92.
[13] B. Dreher J. Friedrich, K. Merle, H. Rothhaas, G. Luhrs, Nucl. Phys., A 235 (1974) 219-248.
[14] G. A. Lalazissis and S. Raman, Atomic Data and Nuclear Data Tables, 71 (1999) 1-40.
[15] M. Wang, G. Audi, A. H. Wapstra, F. G. Kondev, M. M. Cormick, X. Xu, B. Pfeiffer, Chinese Physics, C 36 (2012) 1603-2014.
[16] E. A. Knight, R. P.Singhal, M. W. Macauley, J. Phys., G 7 (1981) 1115-1121.
[17] C. Li, M. R. Yearian, I. Sick, Phys. Rev., C 9 (1974) 1861-1877.